Liquid Crystalline Polyacetylenes: Synthesis and Properties of Poly{*n*-[((4′-cyano-4-biphenylyl)oxy)carbonyl]-1-alkynes}

Ben Zhong Tang,* Xiangxing Kong, Xinhua Wan, Han Peng, and Wing Yip Lam

Department of Chemistry, Hong Kong University of Science & Technology (HKUST), Clear Water Bay, Kowloon, Hong Kong, China

Xin-De Feng

Department of Chemistry, Peking University, Beijing 100871, China

Hoi Sing Kwok

Department of Electrical & Electronic Engineering and Center for Display Research, HKUST, Clear Water Bay, Kowloon, Hong Kong, China

Received November 13, 1997; Revised Manuscript Received February 3, 1998

ABSTRACT: It is generally believed that cyano functionality is "toxic" to the classical $MoCl_5$- and WCl_6-based metathesis catalysts, but we here present such an example in which a group of cyano-containing acetylene monomers are polymerized by the "simple" metal halides. The $WCl_6(-Ph_4Sn)$ catalysts in dioxane initiate the polymerizations of *n*-{[(4′-cyano-4-biphenylyl)oxy]carbonyl}-1-alkynes (**AnCN**; n = 2, 3, 8), yielding polymers (**PAnCN**s) with relatively narrow molecular weight distributions (M_w/M_n down to 1.3). The same metal−halide mixtures in toluene, however, are generally ineffective in polymerizing **AnCN**s, suggesting that the tungsten−oxo complexes are involved in the active center formation. The differential scanning calorimetry, polarizing optical microscopy, and X-ray diffractometry analyses reveal that all the **PAnCN**s are mesomorphic, with the longer flexible spacer favoring the better ordering of the mesogenic groups. **PA2CN** shows monotropic nematicity, **PA3CN** exhibits enantiotropic nematicity, and **PA8CN** displays enantiotropic smecticity with an interdigitated molecular packing arrangement (s_{Ad}) over a wide temperature range (ca. 110 °C). In-domain banded structures within the s_{Ad} layers of **PA8CN** are observed during the transit of the bâtonnets to the focal-conic fan textures, and the formation of large scale band morphology is achieved by the application of shear force to **PA8CN** in its liquid crystalline state.

Introduction

Polyacetylene is a prototypical conjugated polymer, and liquid crystals are widely used in modern optical display systems.[1] Attachment of mesogenic pendant groups to the conjugated polyacetylene backbone is of interest because the resulting polymers may possess intriguingly unique electrical and optical properties. The polymers, for example, may be both electrically conductive and liquid crystalline. They may also be both second- and third-order nonlinear optically susceptible because conjugated π-electron systems are $\chi^{(3)}$-active and polarized mesogenic groups are $\chi^{(2)}$-active.[2] Recently, it has been found that some conjugated polymers and liquid crystals effectively limit strong optical pulses,[3] and the liquid crystalline polyacetylenes thus may show superior optical limiting performance.

Almost all the side-chain liquid crystalline polymers prepared so far possess flexible polymer backbones, and those possessing rigid backbones have seldom been synthesized.[1] Development of liquid crystalline polymers with rigid polyacetylene backbones thus may open up new avenues for exploring new types of liquid crystalline polymers and widen our understanding on liquid crystal molecules. Because of the orientability of stiff-chain polymers by external forces, the liquid crystalline polyacetylenes may exhibit anisotropic mechanical properties, which may contribute to the search for high-performance engineering materials.

Notwithstanding the attractive potential, synthesis of liquid crystalline polyacetylenes remains a virtually unexplored research area.[4] The difficulty lies in the seemingly incompatible nature of the polar functional groups in the liquid crystalline mesogens with the commonly used transition-metal catalysts for the acetylene polymerizations.[5] Akagi and Shirakawa have recently succeeded in the polymerization of a group of mesomorphic acetylene monomers containing an ether functionality and found that the electrical conductivity of a magnetically aligned liquid crystalline polyacetylene increased about 2 orders of magnitude in the direction parallel to the magnetic field.[6] Incorporation of mesogenic groups with cyano tails into the polyacetylene chains is of particular interest because of the strong polarizability of the cyano tails and the large electrical-field susceptibility of the polarized mesogenic groups. Polymerization of the cyano-containing acetylene monomers, however, has been a daunting task. The polymerizations of cyanoalkynes such as propionitrile (HC≡CCN) and 5-cyano-1-pentyne [$HC{\equiv}C(CH_2)_3CN$] initiated by $MoCl_5-Ph_4Sn$ gave either a few percent insoluble black powdery substance or oligomers with molecular weights of a few thousand.[7]

In our previous work, we tried to tackle the problem.[8] We designed and synthesized a group of acetylene monomers containing the cyano functionality, {4-[((*n*-((4′-cyano-4-biphenylyl)oxy)alkyl)oxy)carbonyl]phenyl}-acetylene (**BnCN**). As anticipated, the polymerization of **BnCN** was not easy, and our attempts to initiate the acetylene polymerization by the classical $MoCl_5$- and WCl_6-based catalysts all ended in disappointments. We

S0024-9297(97)01672-0 CCC: $15.00
Published on Web 03/25/1998

Chart 1

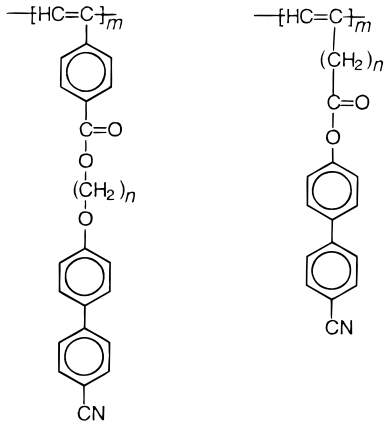

PBnCN (n = 6, 12) **PAnCN** (n = 2, 3, 8)

Scheme 1

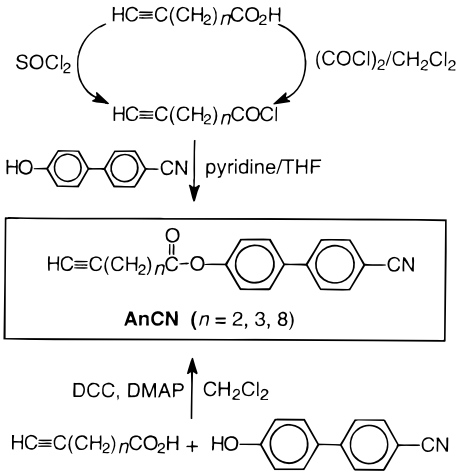

eventually succeeded in converting the monomers to high molecular weight, stereoregular polymers (**PBnCN**; Chart 1) using an organorhodium complex, $[Rh(nbd)Cl]_2$, as the polymerization catalyst.[8] Unfortunately, however, the polymers were not mesomorphic, even when the length of the flexible spacer was as long as 12 methylene units. Krongauz and co-workers have found that the polyacrylates containing spiropyran side groups undergo swelling-induced crystallization but their polystyrene counterparts do not, due to the rigidity of the polystyrene main chain.[9] Grubbs' group compared the mesomorphic behavior of two side-chain liquid crystalline polymers with different backbone rigidity and demonstrated that the more rigid the polymer backbone, the less ordered the mesogenic units.[10] We thus suspect that the nonmesomorphism of **PBnCN**s is due to the high rigidity of the poly(phenylacetylene) backbone.

The polyalkyne backbones consisting of alternating double bonds $[-(CH{=}CR)_n-]$ are much more rigid than the polyalkene backbones consisting of single bonds $[-(CH_2{-}CHR)_n-]$, as reflected by the fact that the glass transition temperature (T_g) of polyacetylene $[-(CH{=}CH)_n-]$ is much higher than that of polyethylene $[-(CH_2{-}CH_2)_n-]$ ($\Delta T_g > 275$ °C!).[11] This, however, does not necessarily imply that the stiffness of the polyalkyne main chains cannot be manipulated by varying the kinds of the substituent pendant (R), as commonly practiced in the molecular design of vinyl-polymer liquid crystals.[1] In this work, we tried to fine-tune the rigidity of polyacetylene backbones by a molecular engineering approach, in an effort to develop the cyano-containing liquid crystalline polyacetylenes.

Although the numbers of the carbon atoms in the repeat units of poly(1-chloro-1-octyne) $\{-[CCl{=}C(n\text{-}C_6H_{13})]_n-\}$ and poly(1-chloro-2-phenylacetylene) $[-(CCl{=}CPh)_n-]$ are the same (8), the T_g of the former (150 °C) is lower than that of the latter (≥200 °C),[11] suggesting that the backbone of a polyacetylene containing an aliphatic substituent ("aliphatic polyacetylene") is somewhat less rigid than that of a polyacetylene containing an aromatic substituent ("aromatic polyacetylene"). Because **PBnCN**s can be regarded as aromatic polyacetylenes, we envision that the main chains of their aliphatic polyacetylene counterparts may be less stiff. We thus designed a group of aliphatic alkynes, *n*-{[(4′-cyano-4-biphenylyl)oxy]carbonyl}-1-alkynes (**AnCN**), in which the flexible methylene spacers are directly linked to the acetylene triple bond instead through a phenyl ring.

Polymerization of **AnCN**, however, might be quite challenging. Organorhodium complexes are tolerant of many functional groups[8,12] but are not effective catalysts for the polymerizations of aliphatic alkynes. The molybdenum and tungsten catalysts are effective for the polymerizations of nonpolar aliphatic alkynes[4] but may be poisoned by the polar cyano group in **AnCN**.[7,8] In this paper, we report our efforts in polymerizing the polar cyanoalkyne monomers and present the mesomorphic properties of the resulting cyano-containing polyacetylenes (**PAnCN**).

Results and Discussion

Monomer Synthesis. We prepared the cyanoalkyne monomers **AnCN**s by esterification of *n*-alkynoic acids with a mesogenic alcohol, 4′-hydroxy-4-biphenylcarbonitrile (Scheme 1). The esterification was achieved by a two-step reaction: the acids were allowed to react with neat thionyl chloride or oxalyl chloride/dichloromethane solution in the first step, followed by the reaction of the resulting acid chlorides with the mesogenic alcohol in the second step.[13] The esterification was also accomplished by direct condensation of the alkynoic acids with the mesogenic alcohol in the presence of 1,3-dicyclohexylcarbodiimide (DCC), a dehydrating agent, and 4-(dimethylamino)pyridine (DMAP), a strong base.[14] Because of the simplicity (one pot and one step), most samples of the **AnCN**s used in this study were prepared by the direct condensation reaction. All the reactions gave the esterification products in high isolation yields (>70%). The products were purified by column chromatography followed by recrystallization. We characterized the purified products by standard spectroscopic methods and obtained satisfactory analysis data (see Experimental Section).

All the **AnCN** monomers were white crystals at room temperature and showed no liquid crystallinity at elevated temperatures before melting to an isotropic liquid. We determined the crystal structures of the **A2CN** and **A8CN** single crystals by X-ray diffraction analysis and found that the molecules were regularly packed in layered structures, in which the acetylene heads and the cyano tails were held together via intermolecular hydrogen bonds, $-C{\equiv}C{-}H{\cdots}N{\equiv}C-$.[15] The layers of the **A8CN** molecules were interdigitated in an antiparallel fashion and the interlayer interaction

Table 1. Polymerization of 5-{[(4′-Cyano-4-biphenylyl)oxy]carbonyl}-1-pentyne (A3CN)[a]

			polymers		
no.	catalyst	solvent	yield (%)	M_w[b]	M_w/M_n[b]
1	$MoCl_5$	toluene	0		
2	$MoCl_5-Ph_4Sn$	toluene	8.2	4 800	2.2
3	$MoCl_5$	THF	0		
4	$MoCl_5-Ph_4Sn$	THF	0		
5	WCl_6	toluene	0		
6	WCl_6-Ph_4Sn	toluene	8.0	2 900	1.4
7[c]	WCl_6	THF	31.2	25 100	1.7
8[c]	WCl_6-Ph_4Sn	THF	49.0	20 200	1.6
9	WCl_6-Ph_4Sn	dioxane	62.1	22 300	1.6

[a] Polymerized under nitrogen at room temperature for 24 h; $[M]_0$ = 0.2 M, [cat.] = ([cocat.] =) 20 mM. [b] Determined by GPC on the basis of a polystyrene calibration. [c] For the **PA3CN** fraction only. The poly(THF) fraction was removed by repeated precipitation (see text for details).

between the negatively charged nitrogen in the cyano group and the positively charged oxygen in the phenoxy group was clearly observed.

Polymerization Reactions. We attempted to polymerize **AnCN**s using the $[Rh(nbd)Cl]_2$ complex but failed to obtain any isolable polymeric products. Akagi and Shirakawa polymerized their mesomorphic acetylene monomers such as 5-[(4′-pentyl-4-biphenylyl)oxy]-1-pentyne [HC≡C$(CH_2)_3$O-biph-C_5H_{11}; biph = biphenyl] in toluene using $MoCl_5-Ph_4Sn$ as the catalyst.[6] We thus tried to polymerize our cyano-containing pentyne monomer **A3CN** using the similar reaction conditions. The reaction catalyzed by $MoCl_5$ in toluene, however, gave no polymeric products (Table 1, no. 1). Adding the Ph_4Sn cocatalyst to the reaction system did not help much: an oligomeric species with a M_w of 4800 was isolated in a few percent yield after a 24-h polymerization. The attempted polymerizations in THF using the Mo catalysts were also unsuccessful. The difference between Akagi's and our monomers is the polarity of the functional groups: Akagi's monomer contains a less polar ether group, whereas our monomer contains more polar ester and cyano groups.[16,17] Taking into consideration that the polymerizations of methyl propiolate [HC≡CCO_2CH_3][18] and 5-cyano-1-pentyne [HC≡C$(CH_2)_3$-CN][7] catalyzed by $MoCl_5-Ph_4Sn$ gave only oligomeric products, the failure in polymerizing **A3CN** may be due to the poisoning interaction of the polar ester and cyano groups with the Mo-based catalyst systems. $WCl_6(-Ph_4$-Sn) are known to be effective catalysts for the polymerizations of phenylacetylene derivatives with ester groups (HC≡CC_6H_5-*p*-CO_2R) in toluene.[19] The reaction of **A3CN** catalyzed by WCl_6 in toluene, however, yielded no polymeric products, and the polymerization initiated by WCl_6-Ph_4Sn gave only 8% of an oligomeric species (Table 1, nos. 5 and 6).

The reaction in THF, however, was encouraging: After **A3CN** and WCl_6 were admixed in THF, the color of the reaction mixture changed from red brown to green in a few minutes. The viscosity increased very fast and the polymerization solution could not be stirred by the magnetic bar in ca. 30 min. After 24 h, we dissolved the reaction product in THF, poured the dilute THF solution into methanol, and isolated the precipitate by filtration. The gel permeation chromatography (GPC) analysis of the product, however, gave two RI peaks, although the UV detector recorded virtually only one peak (Figure 1A). Since the working wavelength of the UV detector was 254 nm, the fact that the sharp RI peak

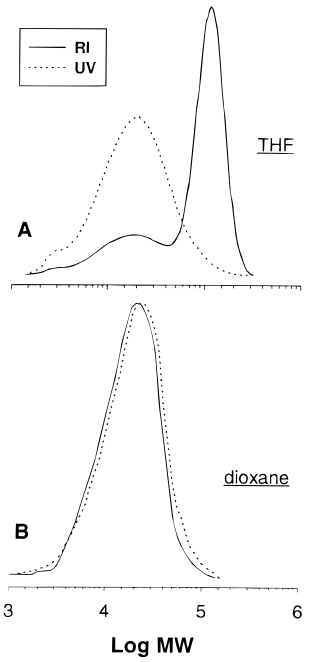

Figure 1. GPC traces of polymerization products of **A3CN** catalyzed by (A) WCl_6 in THF (sample from Table 1, no. 7) and (B) WCl_6-Ph_4Sn in dioxane (Table 1, no. 9).

in the high molecular weight region had no corresponding UV−GPC peak indicates that the high molecular weight fraction contains no aromatic chromophores. In other words, the fraction should not be the polymer of **A3CN** but might be the polymer of the THF solvent.[20] It is known that poly(THF) is soluble in methanol, and we thus redissolved the reaction product in chloroform and reprecipitated the polymer solution into methanol. We repeated the dissolution−precipitation process many times and eventually suppressed the UV-insensitive RI−GPC peak to under the detection limit of the RI detector. The suppression of the RI peak by the precipitation in methanol thus confirms that the high molecular weight fraction is indeed poly(THF). It is noteworthy that, both being Lewis acids, WCl_6 initiated the THF polymerization but $MoCl_5$ failed to do so (cf. Table 1, no. 3). The sharp RI peak in the high molecular weight region gave a polydispersity index (M_w/M_n) close to unity, suggesting that the WCl_6-initiated polymerization of THF is living in nature. The precipitate after the repeated precipitation was isolated in ca. 30% yield (Table 1, no. 7). The GPC analysis of the precipitate gave only one RI peak and one corresponding UV peak with a polystyrene-calibrated M_w of 25 100. The precipitate was insoluble in methanol and characterizable by the UV detector, which thus should be the polymer of **A3CN** (or **PA3CN**). It becomes clear that WCl_6 can polymerize **A3CN** in THF, albeit with the complication of the simultaneous ring-opening polymerization of the solvent. Similar results were obtained when WCl_6-Ph_4-Sn was used as the catalysts; that is, the polymerizations of **A3CN** and THF were simultaneously initiated. The addition of the Ph_4Sn cocatalyst increased the polymer yield but somewhat decreased its M_w (Table 1, no. 8).

To eliminate the complication of the solvent polymerization and to obviate the trouble of separating the large amount of the byproduct of the solvent polymer, we tried to use dioxane as the polymerization solvent. Unlike its THF cousin, dioxane is resistant to ring-

Table 2. Polymerization of 10-{[(4′-Cyano-4-biphenylyl)oxy]carbonyl}-1-decyne (A8CN)[a]

				polymers		
no.	catalyst[b]	temp (°C)	solvent	yield (%)	M_w[c]	M_w/M_n[c]
1	$MoCl_5$	rt	THF	0		
2	$MoCl_5-Ph_4Sn$	rt	toluene	12.0	18 400	1.6
3	$MoCl_5-Ph_4Sn$	rt	dioxane	5.1	23 500	1.7
4	$MoCl_5-Ph_4Sn$	80	dioxane	0		
5	WCl_6	rt	toluene	0		
6[d]	WCl_6	rt	THF	15.0	24 900	2.0
7[d]	WCl_6-Ph_4Sn	rt	THF	46.1	38 700	2.9
8	WCl_6	rt	dioxane	56.3	23 400	1.8
9	WCl_6-Ph_4Sn	rt	dioxane	22.0	36 100	2.2
10	WCl_6-Ph_4Sn	80	dioxane	46.8	40 500	1.8
11	$W(mes)(CO)_3$	rt	CCl_4	0		
12	$W(mes)(CO)_3$	60	CCl_4	36.0	30 900	1.6
13	$Mo(nbd)(CO)_4$	rt	CCl_4	30.8	13 200	2.1
14	$Mo(nbd)(CO)_4$	60	CCl_4	15.9	11 200	1.6

[a] Polymerized under nitrogen for 24 h; $[M]_0 = 0.2$ M, [cat.] = ([cocat.] =) 20 mM. [b] mes = mesitylene, nbd = 2,5-norbornadiene (or bicyclo[2.2.1]hepta-2,5-diene). [c] Determined by GPC on the basis of a polystyrene calibration. [d] For the **PA8CN** fraction only. The poly(THF) fraction was removed by repeated precipitation (see text for details).

Table 3. Polymerization of 4-{[(4′-Cyano-4-biphenylyl)oxy]carbonyl}-1-butyne (A2CN)[a]

			polymers		
no.	catalyst[b]	temp (°C)	yield (%)	M_w[c]	M_w/M_n[c]
1	$MoCl_5$	rt	0		
2	$MoCl_5$	80	30.4	4 400	1.5
3	$MoCl_5-Ph_4Sn$	rt	41.0	31 400	2.2
4	$MoCl_5-Ph_4Sn$	80	54.0	3 800	1.5
5	WCl_6	rt	34.9	20 300	1.8
6	WCl_6	80	38.5	19 200	2.3
7	WCl_6-Ph_4Sn	rt	32.8	11 800	1.3
8	WCl_6-Ph_4Sn	80	33.5	21 700	2.3
9	WCl_6-MPO	rt	21.4	13 100	1.4
10	WCl_6-Ph_4Sn-MPO	rt	22.7	11 000	1.5

[a] Polymerized in dioxane under nitrogen for 24 h; $[M]_0 = 0.2$ M, [cat.] = ([cocat.] =) 20 mM. [b] MPO = 4-methoxyphenol. [c] Determined by GPC on the basis of a polystyrene calibration.

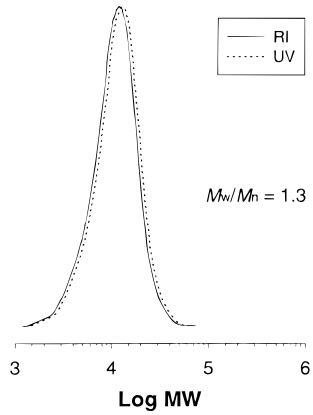

Figure 2. GPC trace of polymerization product of **A2CN** catalyzed by WCl_6-Ph_4Sn in dioxane (sample from Table 3, no. 7).

opening polymerization because of its stable six-membered ring structure.[21] When dioxane was used as solvent, the red brown color of the polymerization mixture remained unchanged and the solution could be stirred during the whole course of the reaction, suggesting that the dioxane solvent does not undergo the undesired polymerization reaction. After a 24-h reaction, a red-brown powder was isolated in 62.1% yield (Table 1, no. 9). The GPC analysis of the product gave only one UV-sensitive RI peak (Figure 1B), confirming that the polymerization system is much "cleaner" and that the dioxane solvent had not complicated the acetylene polymerization.

The polymerization behavior of **A8CN**, which has a longer methylene spacer, was similar to that of **A3CN** and can be briefly summarized as follows: (i) WCl_6-Ph_4Sn is a good catalyst, (ii) toluene is not a good solvent, and (iii) dioxane gives cleaner results (Table 2).

In 1989, Tang and Kotera found that some organomolybdenum and -tungsten complexes such as $M(CH_3CN)_3(CO)_3$ and $M(mes)(CO)_3$ (where M = Mo, W; mes = mesitylene) were effective catalysts for acetylene polymerizations.[22] Because $W(mes)(CO)_3$ is very stable and can be handled in an open atmosphere, we tried to use it to polymerize **A8CN**. The reaction carried out in carbon tetrachloride at room temperature failed but the polymerization at 60 °C yielded a high molecular weight polymer (M_w 30 900) with a low polydispersity (M_w/M_n 1.6; Table 2, nos. 11 and 12). Interestingly, although $MoCl_5$ was not a good catalyst, the $Mo(nbd)(CO)_4$ complex initiated the polymerization of **A8CN** even at room temperature. Different from the temperature effect of $W(mes)(CO)_3$, increasing the polymerization temperature decreased the catalytic efficiency of $Mo(nbd)(CO)_4$. Although the polymers obtained from the polymerization reactions catalyzed by the organomolybdenum and -tungsten complexes were stable at room temperature, they gradually darkened upon heating. Because Mo and W carbonyls can form complexes with nitrile and arene,[22,23] the darkening might be due to the decomposition of the organometallic complexes formed between the metal carbonyls and the cyano and/or phenyl groups of the acetylene polymers during the polymerization reactions. Although the formation and decomposition of the polymer−metal complexes are of interest in terms of developing polymer-supported organometallic catalysts and polymer-dispersed metal nanoclusters, the darkening of the polymers at high temperatures frustrated our efforts in investigating their mesomorphic properties. We thus did not further study the catalytic properties of the $W(mes)(CO)_3$ and $Mo(nbd)(CO)_4$ complexes in this work.

It has become apparent that toluene is a "bad" solvent for the cyanoalkyne polymerization and THF invites the complication of the solvent polymerization. We thus investigated the polymerization behavior of **A2CN**, which has a short methylene spacer length, in dioxane only. The reactions catalyzed by $MoCl_5$ at room temperature and 80 °C both failed to produce high molecular weight polymers (Table 3, nos. 1 and 2). Surprisingly, a polymer with an M_w of 31 400 was isolated in 41% yield when $MoCl_5-Ph_4Sn$ was used as the catalyst at room temperature, although the catalyst gave only 5.1% of **PA8CN** under identical polymerization conditions. Increasing the reaction temperature increased the polymer yield but decreased its M_w. All the $WCl_6(-Ph_4Sn)$ catalysts polymerized **A2CN**, with the polymers obtained from the room-temperature (rt) reactions possessing lower polydispersities (Table 3, nos. 5 and 7). The GPC peak of the polymer isolated from the WCl_6-Ph_4Sn/rt system was very sharp (Figure 2), and optimization of the reaction conditions may lead to the

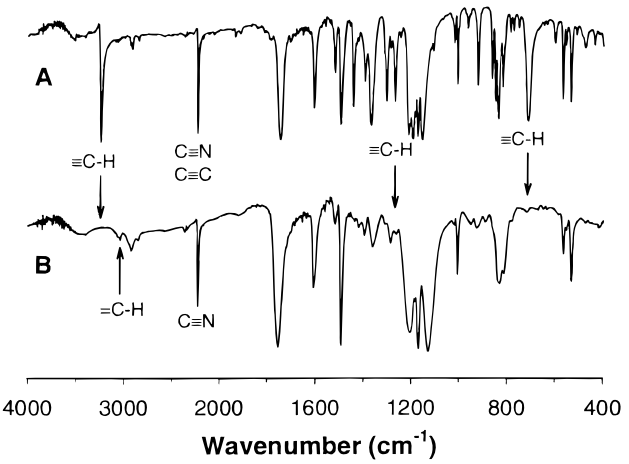

Figure 3. IR spectra of (A) **A2CN** and (B) **PA2CN** (sample from Table 3, no. 7).

development of living acetylene polymerization systems. Masuda et al. found that addition of a trace amount of alcohol to Mo-based catalysts improved the "livingness" of certain acetylene polymerization systems.[24] We thus added an alcohol, 4-methoxyphenol (MPO), to the W catalyst systems. The molecular weights and polydispersities of the resulting polymers, however, were hardly affected by the addition of the alcohol (cf. Table 3, nos. 7, 9, and 10).

Structural Characterization. All the purified polymerization products gave satisfactory spectroscopic data corresponding to their expected molecular structures. A typical example of the IR spectra of the polymers is shown in Figure 3B. The absorption bands of **A2CN** at 3244, 1305, and 710 cm^{-1} originating from the ≡C−H stretching and bending vibrations all disappeared in the spectrum of **PA2CN**. Compared with the monomer, the relative intensity of the band at 2231 cm^{-1} vs that at 1746 cm^{-1} in the spectrum of **PA2CN** decreased, due to the conversion of the triple bond of the monomer to the double bond of the polyacetylene backbone by the polymerization reaction. The absorption band of the =C−H stretching appeared as a new weak band at 3040 cm^{-1}. The disappearance of the bands related to the propargyl (≡C−CH_2) vibrations at 1443 (scissoring), 1305 (wagging; overlapping with the bending overtone of ≡C−H), 1270 (twisting), and 922 cm^{-1} (C−C stretching)[25] further corroborates that the monomer had undergone the acetylene polymerization.

The NMR analysis provided valuable information on the stereostructure of the resulting polyacetylenes. As shown in Figure 4B, in the ^{1}H NMR spectrum of the **PA2CN** prepared by the $MoCl_5$−Ph_4Sn catalyst, there was no peak in the acetylene proton absorption region (ca. δ 2.0). Instead, a new peak appeared in the olefin region (δ 5.8−6.5), which was absent in the spectrum of **A2CN** (Figure 4A). Masuda and Higashimura reported that the cis olefin proton of an aliphatic poly(1-alkyne), poly(3,3-dimethyl-1-pentyne) {−[HC=C(CMe_2-CH_2CH_3)]$_n$−}, absorbed at δ 6.05.[26] Because **PA2CN** can be viewed as a derivative of an aliphatic poly(1-alkyne) {−[HC=C(CH_2CH_2R)]$_n$−, where R is the [(cyanobiphenylyl)oxy]carbonyl group}, it seems reasonable to assign the peak centered at δ 6.26 to the absorption by the cis olefin proton in the alternating-double-bond backbone of **PA2CN**. The absorption peaks of the trans proton of monosubstituted polyacetylenes are normally located in the region where aromatic protons absorb (>δ 6.7).[8,27] Integration of the peak areas (A) in the aromatic (a) and olefin (o) regions gave a ratio of A_a/A_o = 8.0/0.7 (or 11.4/1.0), confirming that the trans proton of **PA2CN** absorbs in the aromatic region. By analogy to the equations used by Percec[27a,b] and us[8,28] for evaluating the stereostructures of the poly(phenylacetylene) derivatives, we used the following equation to calculate the cis content of **PA2CN**:

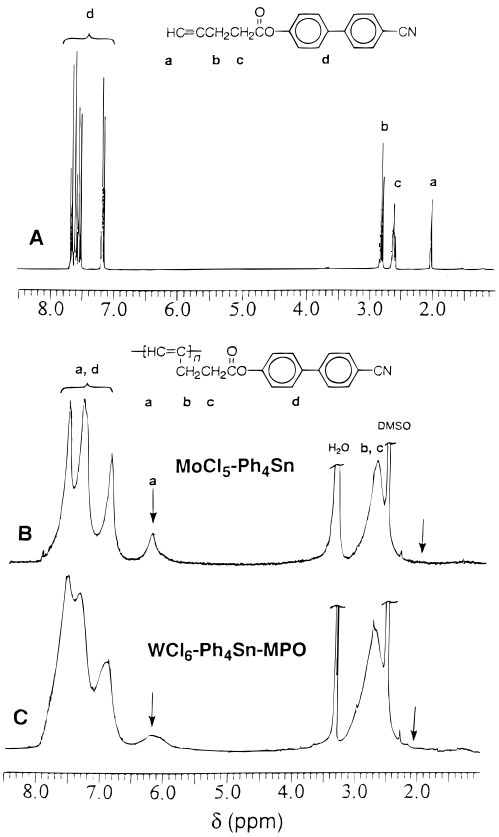

Figure 4. ^{1}H NMR spectra of (A) **A2CN** (in chloroform-d) and its polymers **PA2CN** (in DMSO-d_6) prepared using (B) $MoCl_5$−Ph_4Sn (sample from Table 3, no. 3) and (C) WCl_6−Ph_4Sn-MPO (Table 3, no. 10) as the catalysts.

$$\text{cis content (\%)} = \{A_{6.26}/[(A_a + A_o)/9]\} \times 100 \quad (1)$$

where $A_a + A_o = A_{7.61} + A_{7.37} + A_{6.93} + A_{6.26}$. The cis content thus obtained was 72.4%, close to the value (77%) estimated by Masuda and co-workers[29] by the ^{13}C NMR analysis of the poly(1-butyne) {−[HC=C(CH_2-CH_3)]$_n$−} prepared by $MoCl_5$ [noting that from the molecular structure point of view, **PA2CN** is a derivative of poly(1-butyne)].

The spectrum of the **PA2CN** obtained from the W catalyst (Figure 4C) was similar to that of the polymer prepared by the Mo catalyst. Its cis content estimated by eq 1, however, was lower (61.4%). When a polymer consists of comparable amounts of cis and trans stereoisomers, it normally gives relatively broad absorption peaks because the absorbing species in the different stereochemical environments would have different chemical shifts.[30,31] The absorption peaks of the W polymer were indeed broader, supportive of its lower cis content estimated by eq 1.

The olefin proton absorption of **PA8CN** differed from that of **PA2CN** in both position and intensity. The cis peak of the **PA8CN** prepared by WCl_6−Ph_4Sn in THF centered at δ 5.88 (Figure 5B), a shift of ca. 0.3 ppm

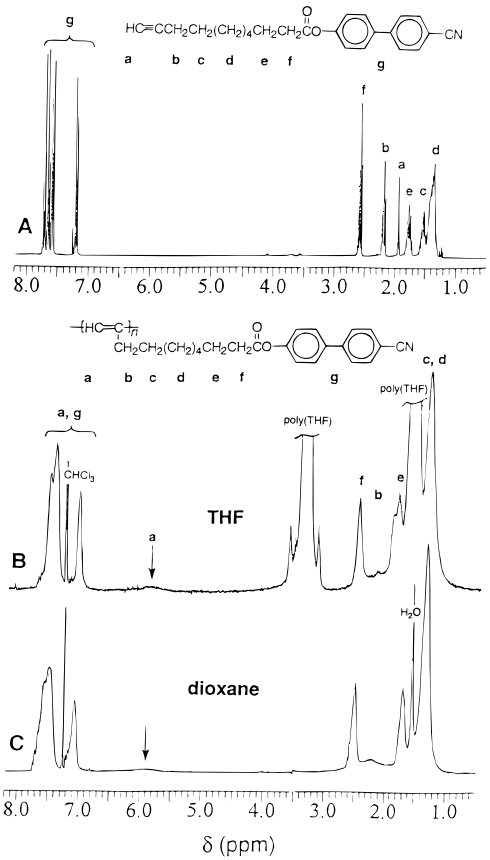

Figure 5. ^{1}H NMR spectra of chloroform-*d* solutions of (A) **A8CN** and its polymers **PA8CN** prepared using WCl_6-Ph_4Sn as the catalyst in (B) THF (sample from Table 2, no. 7) and (C) dioxane (Table 2, no. 9).

from that of **PA2CN**. The upfield shift might be due to the diminution of the deshielding effect of the electron-withdrawing [(cyanobiphenylyl)oxy]carbonyl group, implying that the long alkyl spacer has decoupled the interaction between the polyacetylene backbone and the mesogenic pendants. The intensity of the cis peak was noticeably weak, suggesting that the majority of the olefin protons are in the trans environment or that the polymer is stereochemically trans-rich. The calculation by eq 1 using the integration data in the aromatic and olefin regions (the chloroform peak being carefully excluded) gave a cis content of 24.4% (or a trans content of 75.6%). The predominance of the trans structure brought about good stereoregularity, as reflected by the relatively sharp absorption peaks of the polymer. The as-obtained polymeric product from the polymerization reaction in THF gave huge poly(THF) absorption peaks, which cannot be completely eliminated by the repeated precipitation of the product in methanol. Further studies are under way to clarify whether the product is purely a mixture of the homopolymers of **A8CN** and THF or some sort of copolymer of the two.

The spectrum of the **PA8CN** prepared by the same W catalyst in dioxane was much cleaner (Figure 5C), with no peaks being observed at ca. δ 3.5, where the solvent polymer, if any, would absorb (pure dioxane absorbing at δ 3.55). The NMR data thus confirm the GPC observation that the acetylene polymerization in dioxane is not complicated by the solvent polymerization or that the resulting polyacetylene is not contaminated by the solvent polymer. Like the **PA8CN** prepared in THF, the polymer prepared in dioxane also showed a

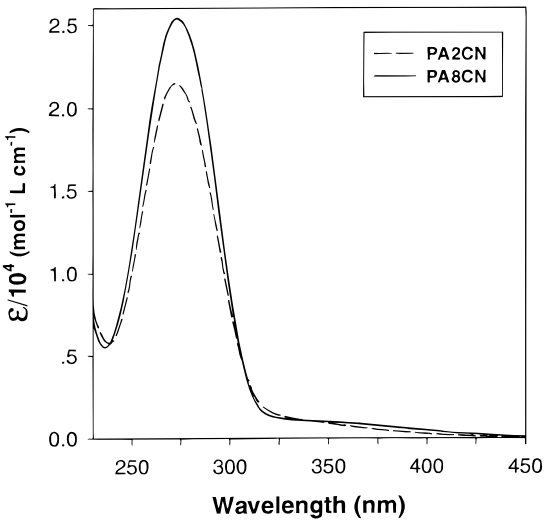

Figure 6. UV spectra of THF solutions of **PA2CN** (sample from Table 3, no. 9) and **PA8CN** (Table 2, no. 9).

weak absorption peak of the cis proton at δ 5.95, implying that the stereostructure of the polymer is again trans-rich. The cis content of the polymer calculated by eq 1 was somewhat higher (36.5%), suggesting that the solvent also plays a role in fine-tuning the stereostructure of the polymer, as observed by Masuda and Higashimura in their acetylene polymerization systems.[26,29,32]

The UV spectra of the poly(cyanoalkynes) showed absorption peaks originating from their alternating-double-bond backbones. While the monomers did not show any absorption peak above ca. 325 nm, the UV spectrum of **PA2CN** well extended to beyond 450 nm (Figure 6). The absorption, however, was quite weak. The steric crowding caused by the bulky mesogenic pendant groups might have forced the neighboring double bonds out of coplanarity, thus reducing the intensity of the absorption by the polyacetylene main chain. The absorption of the [(cyanobiphenylyl)oxy]-carbonyl mesogen peaked at 272.4 nm was 26.4-nm blue-shifted from that of biphenyl (246 nm),[33] indicating that the mesogenic group was polarized. The UV spectrum of **PA8CN** was similar to that of **PA2CN**, except that the absorption peak by the mesogenic chromophore at 273.2 nm was noticeably stronger. When the mesogenic groups are decoupled from the polymer main chain by a long methylene spacer, the reduced steric crowding may allow the biphenyl rings to be more coplanar, thus resulting in the observed hyperchromic effect.

Mesomorphic Properties. By definition, the formation of mesophases of a thermotropic liquid crystalline polymer is realized by the application of heat, and thus thermal stability of the polymer is of primary concern. Because the (unsubstituted) polyacetylene [$-(CH{=}CH)_n-$] readily degrades upon exposure to air at room temperature,[1f] it is of particular importance to check how stable the poly(cyanoalkynes) are.

The poly(1-alkynes) such as poly(1-butyne) and poly-(1-hexyne), which may be regarded as the parent forms of the poly(cyanoalkynes), are so unstable that even the isolation process of the polymer products from the polymerization reactions leads to degradation.[29,34] Thus, the initially precipitated poly(1-alkyne) products in methanol are white and fibrous; they change to yellow powders after drying under vacuum. Poly(1-hexyne)

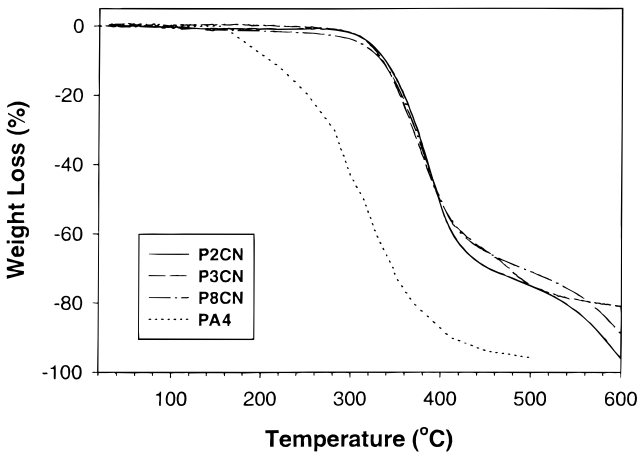

Figure 7. TGA thermograms of mesomorphic polyalkynes **PA2CN** (sample from Table 3, no. 9), **PA3CN** (Table 1, no. 9), and **PA8CN** (Table 2, no. 9) measured under nitrogen at a heating rate of 20 °C/min. The thermogram of a nonmesomorphic polyalkyne **PA4** {poly(1-hexyne) or $-[CH{=}C(CH_2CH_2CH_2H_3)]_n-$} is shown for comparison (data taken from ref 34).

(**PA4**) starts to lose its weight at 150 °C (Figure 7), and heating for a few minutes at the temperature easily changes the yellow powder to a brown gummy fluid.[34] On the other hand, except for the polymerization reactions, which were carried out under an atmosphere of dry nitrogen, all the handlings, including the isolation, purification, and storage of **PAnCN**s, were done in an open atmosphere, during which no any changes in the color and form of the polymer products were observed. As shown in Figure 7, **PA2CN** lost as little as about 1% of its original weight at a temperature as high as 300 °C, at which, **PA4**, the reference polymer without the mesogenic group, lost as much as about half of its original weight. Increasing the length of the flexible methylene spacer did not affect much the thermal stability of the poly(cyanoalkynes), and the weight loss from **PA8CN** at 300 °C remained as low as about 3%. Thus the incorporation of the [(cyanobiphenylyl)oxy]carbonyl mesogen into the pendant group had endowed the polymers with high thermal stability.

The enhanced thermal stability of the poly(cyanoalkynes) may be due to the "jacket effect" of the mesogenic group.[8,35] The alternating-double-bond backbone of the polymers may be surrounded by a rigid "jacket" formed through the intra- and interchain molecular interaction of the mesogenic groups, shielding the polymer main chains from the thermal attack. The polyacetylenes containing aromatic substituents are normally stabler than those containing aliphatic substituents {e.g., thermal stability: $-(HC{=}CPh)_n- \gg -[CH{=}C(CH_2CH_2CH_2H_3)]_n-$[34]}, and thus the energy-sink and radical-trapping functions[3a-d,36,37] of the aromatic mesogens may have also played a role in stabilizing the poly(cyanoalkynes).

After confirming the thermal stability of the polymers by the thermogravimetric analysis (TGA), we investigated their mesomorphic properties. We warmed the **PA2CN** prepared by the W catalyst to its isotropic state by a hot stage in a polarizing optical microscope (POM). Upon cooling, a birefringent texture appeared. A typical microphotograph of the texture is shown in Figure 8A, from which the exact nature of the mesophase is difficult to identify. We repeatedly tried to grow the liquid crystals with care but failed to obtain any photographs with identifiable characteristic mesomorphic textures.

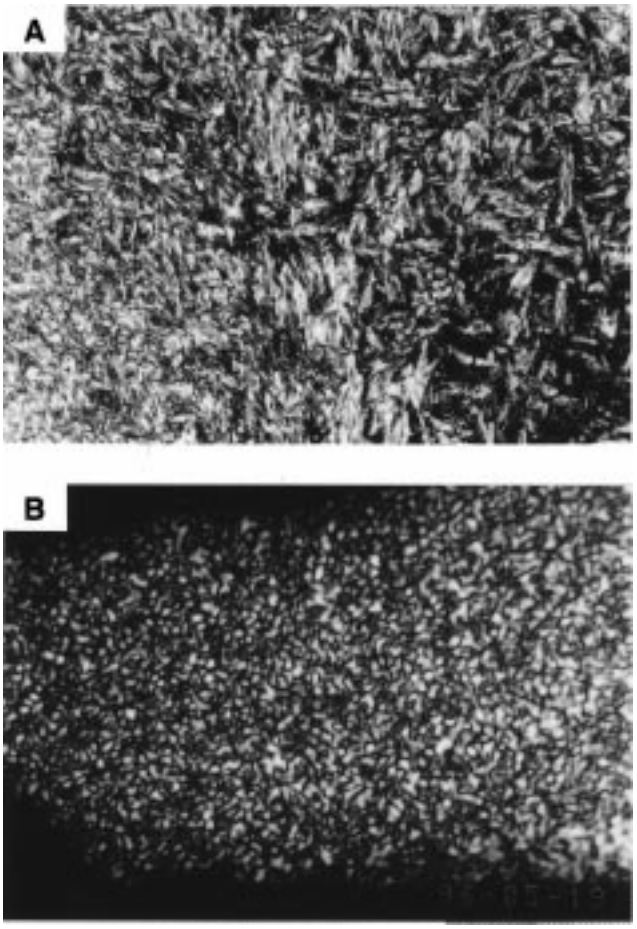

Figure 8. Polarizing optical micrographs (magnification 500×) observed on cooling (A) **PA2CN** (sample from Table 3, no. 7) to 173 °C and (B) **PA3CN** (Table 1, no. 9) to 172 °C from their isotropic states at a cooling rate of 5 °C/min. Annealing time: 2 min. Figure reproduced at 66% for publication.

As revealed by the spectroscopic analysis, the [(cyanobiphenylyl)oxy]carbonyl mesogenic pendants in **PA2CN** were not fully decoupled from the polyacetylene main chain, which may have impeded the growth of the liquid crystals.

We then checked the liquid crystalline properties of the **PA2CN** prepared by the Mo catalyst, which has a higher stereoregularity than the polymer prepared by the W catalyst (cf. Figure 4). In this case, however, we completely failed to observe any mesomorphic textures: The isotropic melt (liquid) between the glass slides remained dark even after it was cooled to the solid state, at which the cover slip could not be sliding anymore. We carefully repeated the observation several times but failed all the time. Thus the stereoregularity of the polymer main chain had a pronounced effect on the mesomorphic properties of the polyacetylene having a short methylene spacer. It is well-known that polymer backbones are a kind of defect distorting the packing of the mesogenic groups and preventing the growth of mesomorphic aggregates. Previous studies on the mesomorphic properties of the poly(meth)acrylates containing biphenyl-based mesogens have revealed that the stereoregular (e.g., isotactic) polymer backbones decrease the stability of the mesophases.[38] For the relatively rigid polyacetylene backbone with a short spacer, the increase in the stereoregularity made the polymer main chains even stiffer, which could not be

offset by the short length of the flexible spacer, thus rendering the polymer completely nonmesomorphic.

When the length of the flexible spacer increased to three methylene units, the polymer exhibited a typical schlieren texture (Figure 8B). Closer examination revealed that the schlieren texture not only showed singularities with four brushes ($s = \pm 1$) but also displayed centers with two brushes ($s = \pm 1/2$). Since the $s = \pm 1/2$ disclinations are not compatible with the s_C mesophase according to Nehring−Saupe theory,[39,40] the schlieren texture thus should be associated with the nematic mesophase of **PA3CN**.

The polymer with an even longer length of methylene spacers (8) showed quite interesting dynamic processes of the mesophase formation. When the isotropic melt of **PA8CN** cooled, mesomorphic textures developed via the nucleation and growth of characteristic bilateral focal-conic entities known as bâtonnets. As shown in the center of Figure 9A, the bâtonnet was evidently growing in a fashion of layer-by-layer addition, following the theoretical treatment on the formation of focal-conic domains of the s_A phase.[40] Interestingly enough, inside the layer, parallel bands normal to the director of the bâtonnet were clearly seen. Upon annealing at 205 °C for another minute, more bâtonnets emerged from the homeotropic dark background, some of which grew and coalesced to form larger domains (noting that the actual domain size in Figure 9B is 2.5 times that in Figure 9A). The banded structures persisted in most of the mesomorphic aggregates, although some of them had lost the fine structure. Further cooling encouraged further growth of the bâtonnets. Coalescence of the domains resulted in the formation of the well-developed characteristic focal-conic fan texture (Figure 9C), which completely buried the banded structures observed in the early stage of the mesomorphic transition.

To check the reproducibility of the banded-structure formation, we repeated the POM observation. When the polymer was slowly cooled from its isotropic state and annealed at 191 °C for 20 min, in addition to the small bâtonnets, a shrimplike domain emerged, in which many parallel bands aligned perpendicular to the director of the domain (Figure 10A). The growth of the domains upon further cooling to 185 °C blurred the banded structures, but closer examination could still find their existence. The banded structures diminished to be observable when the focal-conic fan texture finally evolved. Thus the banded structures were formed by the packing of the mesomorphic layers en route to the focal-conic textures.

The phenomenon of band formation was first observed in mechanically sheared Kevlar fibers in 1977,[41] and since then, the shear-induced banded textures have been identified in a wide range of main-chain liquid crystalline polymers with relatively rigid backbones.[40c,42] We envisioned that shearing **PA8CN** in its liquid crystalline state might facilitate the band formation at larger scale. We thus applied a shear force to the mesomorphic domains of **PA8CN** in its transit to the focal-conic textures. As anticipated, parallel bands formed in the direction perpendicular to the applied shear force (Figure 11). The banded textures have seldom been observed in the "conventional" side-chain liquid crystalline polymers with flexible backbones.[43] The formation of the bands in **PA8CN** thus might be due to the rigidity of its alternating-double-bond backbone.

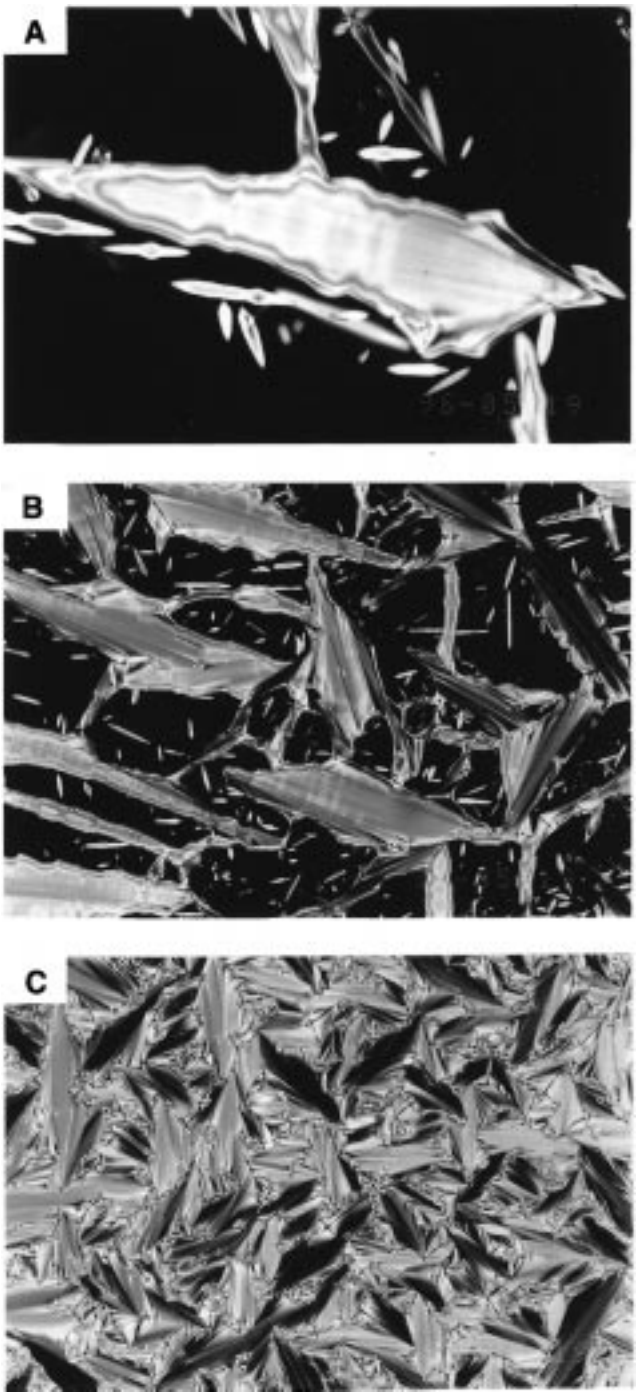

Figure 9. Textures observed on cooling **PA8CN** (sample from Table 2, no. 9) from the isotropic state at a cooling rate of 5 °C/min; microphotographs taken after annealing the sample at 205 °C for (A) 1 min (magnification 500×) and (B) 2 min (200×) and (C) at 170 °C for 2 min (200×). Figure reproduced at 66% for publication.

We carried out X-ray diffraction experiments in order to gain more information on the mesomorphic structures of the polymers and on the molecular packing arrangements within the mesomorphic phases. The samples for the X-ray analysis were prepared by annealing the polymers in their liquid crystalline states, which was then rapidly quenched by liquid nitrogen to freeze the molecular arrangements. The X-ray diffraction diagram of **PA2CN** showed a broad peak in the high-angle region, corresponding to the average intermolecular spacing of ca. 4.4 Å (Figure 12). No reflections were observed at low angles, indicating that there is no layer

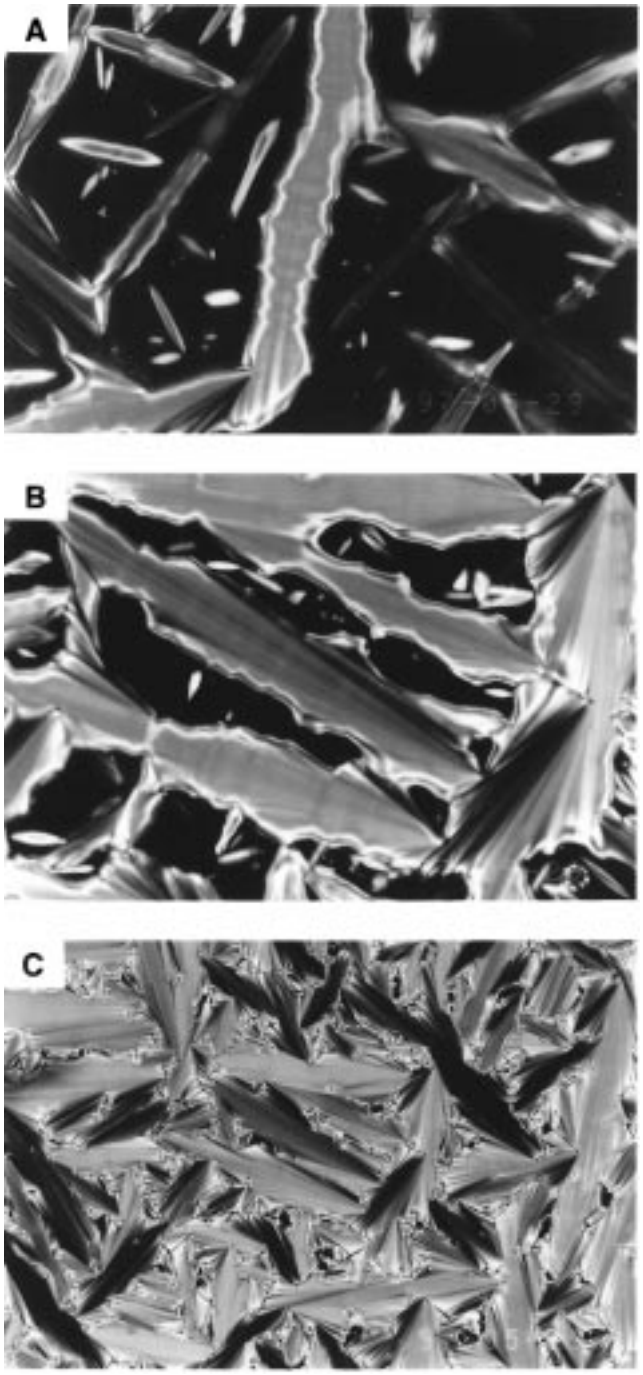

Figure 10. Textures observed on cooling **PA8CN** (sample from Table 2, no. 9) after annealing the sample (A) at 191 °C for 20 min (magnification 500×), (B) at 185 °C for 3 min (500×), and (C) at 175 °C for 5 min (200×). Cooling rate from the isotropic state: 2 °C/min. Figure reproduced at 66% for publication.

ordering within the mesophase. It is known that a nematic mesophase shows only one diffuse halo at high angles.[44] With the help of the X-ray data, we now may assign the texture in Figure 8A to the nematic mesophase of **PA2CN**.

PA8CN, however, showed not only the diffuse peak in the high-angle region, but also Bragg reflections at middle and low angles. The broad hump peaked at $2\theta = 20.7°$ ($d = 4.2$ Å) corresponded to the shorter preferred spacings occurring in the lateral packing arrangement of the alkyl groups within the smectic mesophase.[45] The sharp reflection at $2\theta = 2.7°$ corresponded to a layer

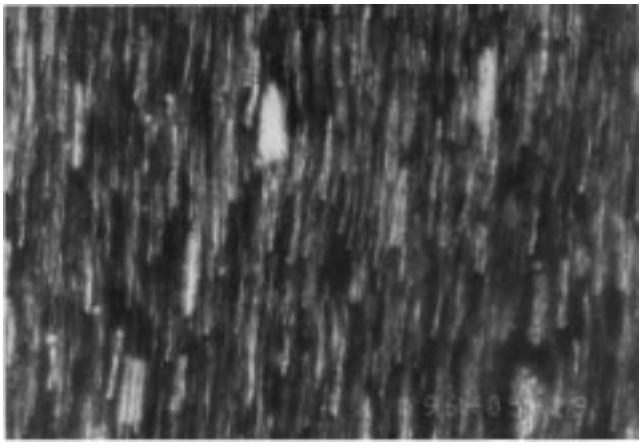

Figure 11. Banded texture (magnification 500×) observed after shearing **PA8CN** (sample from Table 2, no. 9) at 199 °C. Figure reproduced at 66% for publication.

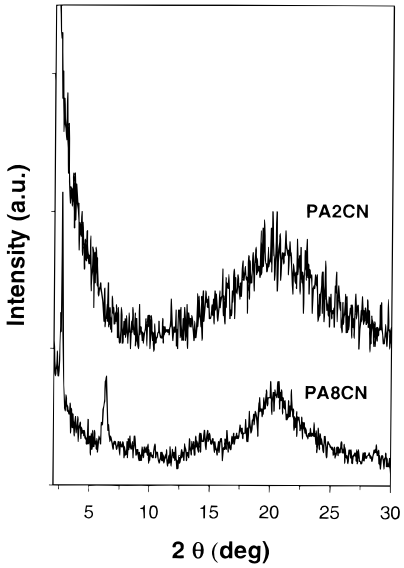

Figure 12. X-ray diffraction patterns of **PA2CN** (sample from Table 3, no. 7) and **PA8CN** (Table 2, no. 9).

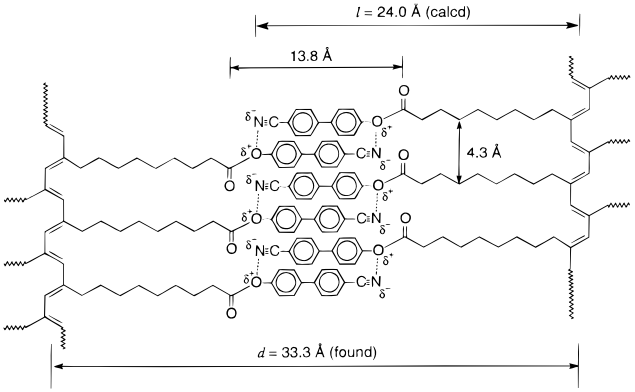

Figure 13. Proposed bilayer packing arrangement of **PA8CN** within the s_A layer with the smectogens interdigitating in a head-to-tail antiparallel fashion.

spacing of 33.3 Å, which is considerably in excess of the molecular length of the repeat unit of **PA8CN** in its most extended conformation ($l = 24.0$ Å). The mesophase of the polymer thus may consist of such a bilayer structure as schematically shown in Figure 13, in which the mesogens arrange in an antiparallel overlapping interdigitated manner, giving a d/l ratio of 1.4, a value often found in the s_{Ad} mesophases of the

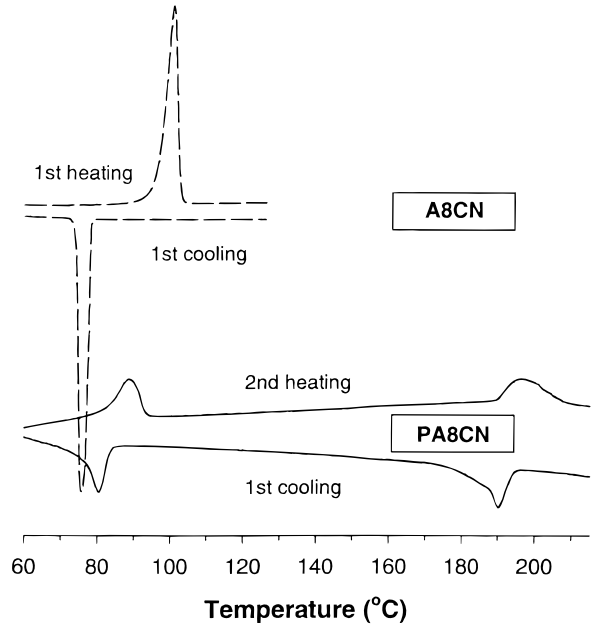

Figure 14. DSC thermograms of **A8CN** and **PA8CN** (sample from Table 2, no. 9) measured under nitrogen at a scanning rate of 10 °C/min.

liquid crystalline molecules containing cyano terminal groups.[38a,46] As revealed by the UV analysis, the [(cyanobiphenylyl)oxy]carbonyl mesogen groups of the polymer were polarized. To minimize the electronic repulsive interactions, partial interdigitation of the polarized mesogens is required. The near-neighbor pairing of the partially negatively charged cyano group with the partially positively charged phenoxy group was actually observed by the X-ray analysis of the single crystals of the monomer (vide ante),[15] further supporting the proposed bilayer packing arrangement of the polymer molecules within the s_A layer.

In the mid-angle region, the diffractogram of the polymer showed a weak reflection at $2\theta = 6.4°$, from which a d spacing of 13.8 Å was derived. Barny et al. also observed the diffuse rings at similar Bragg angles for their cyano-containing polyacrylates $\{-[CH_2CH(CO_2R)]_n-\}$ with different spacer lengths and bridging units: when $R = -(CH_2)_6O$-biph-CN, $d = 12.5$ Å; when $R = -(CH_2)_5CO_2$-biph-CN, $d = 13$ Å.[46a] The calculated length for the interdigitated [(cyanobiphenylyl)oxy]carbonyl groups (or the part between the two carbonyl groups in two adjacent mesogens) in the proposed bilayer structure of **PA8CN** is 13.3 Å. The reflection peak at $2\theta = 6.4°$ thus may be related to the regions in which the polarized rigid [(cyanobiphenylyl)oxy]carbonyl groups are interdigitated and well packed, whereas the order of the flexible octyl spacers is perturbed by the aliphatic chain random motion. The small bump at $2\theta = 14.7°$ ($d = 6.0$ Å) might be the secondary reflection of the mid-angle refraction discussed above.

To estimate the thermodynamic parameters involved in the phase transitions, we conducted differential scanning calorimetry (DSC) analysis. Examples of the DSC thermograms are shown in Figure 14. **A8CN** showed sharp melting and crystallization peaks at 100.7 and 75.7 °C, respectively, during the heating and cooling scans. Its polymer, however, exhibited not only a melting transition at 85.6 °C but also an isotropization transition at 192.5 °C during the second heating scan, giving a mesomorphic temperature range as wide as over 100 °C. The transition peaks recorded during the first cooling scan were approximately in the mirror image of those recorded during the heating scan with a slight shift to the lower temperatures, demonstrating the enantiotropic nature of the phase transitions.

Table 4 summarizes the phase transitions of the cyanoalkyne monomers and their polymers. The melting/crystallization of the **A2CN** crystal/liquid involved large enthalpy and entropy changes (Table 4, no. 1), indicating that the hydrogen-bonding ($-C\equiv C-H\cdots N\equiv C-$) is quite strong and that the monomer molecules are well packed. When the length of the methylene units increases by 1 to 3 (odd number of carbon atoms), all the T_m, ΔH, and ΔS tended to decrease. A further increase of the spacer length to 8 (even number of carbon atoms) appeared to increase, instead of decrease, T_m and corresponding ΔH and ΔS. The odd−even alternation might be due to the better packing of the molecules with the even numbers of methylene units.

The DSC analysis of **PA2CN** failed to detect any thermal transitions during the heating scan but recorded a nematic−isotropic transition at ca. 180 °C during the cooling scan (Table 4, no. 4). The nematic mesophase was identified on the basis of the POM observation and X-ray analysis, and the small ΔH and ΔS values obtained from the DSC analysis further support the mesophase assignment. The nematic mesophase was monotropic and the crystallization transition was not observed during the cooling scan. The perturbation of the polyacetylene backbone did not even allow the mesophase to fully develop into a typical nematic texture (cf. Figure 8A), and it is thus understandable why the mesogenic molecules could not be packed into the crystal lattice.

The nematic mesophase of **PA3CN**, however, was enantiotropic. The phase transition was again characterized by the small enthalpy and entropy changes. The length of the methylene spacer, however, was still not long enough to enable the observation of the melting and crystallization transitions by DSC. The melting/crystallization transitions were observed in **PA8CN** (Table 4, no. 6). The ΔH and ΔS for the k−s_{Ad} transitions, however, were much smaller that those involved in the k−i transitions of its monomer (cf. Table 4, no. 3), partly due to the imperfect feature of the polymer crystals and partly because of the packing order in the s_{Ad} phase. The ΔH and ΔS for the s_{Ad}−i transitions were understandably higher than those for the n−i transitions (cf. Table 4, nos. 4 and 5), because of the stronger molecular interactions and better packing order in the interdigitated smectic A mesophase.

Concluding Remarks

In this study, we succeeded in polymerizing a group of acetylene monomers containing [(cyanobiphenylyl)oxy]carbonyl mesogens with different methylene spacers using simple metal halide catalysts. There are several noteworthy unusual features in the polymerization system: (i) Akagi et al. used $MoCl_5-Ph_4Sn$ to initiate the polymerizations of their mesogenic alkynes containing an ether funtionality,[6] but in our cyanoalkyne polymerizations, the W catalysts are generally superior to their Mo cousins. (ii) Toluene is the most commonly used solvent for acetylene polymerizations[4] but is a bad solvent for the cyanoalkyne polymerizations. (iii) Masuda et al. found that the stereostructure of poly(1-

Table 4. Phase Transitions and Corresponding Thermodynamic Parameters of AnCNs and PAnCNs[a]

		T, °C (ΔH, kJ·mol^{-1}; ΔS, J·mol^{-1}·K^{-1})	
no.	***n***	heating[b]	cooling[c]
		A*n*CN (Monomer)	
1	2	k 157.2 (40.4; 93.9) i	i 135.9 (−35.1; −85.8) k
2	3	k 94.6 (30.3; 82.4) i	i 79.1 (−30.5; −86.6) k
3	8	k 100.7 (39.3; 105.4) i	i 75.7 (−39.4; −112.9) k
		PA*n*CN (Polymer)	
4	2		i 179.6 (−0.6; −1.3) n
5	3	n 210.1 (0.7; 1.4) i	i 188.6 (−0.6; −1.4) n
6	8	k 85.6 (1.2; 3.3) s_{Ad} 192.5 (1.1; 2.4) i	i 190.3 (−1.3; −2.7) s_{Ad} 80.6 (−1.2; −3.3) k

[a] Measured by DSC under nitrogen at a heating or cooling rate of 10 °C/min. Code: k, crystalline state; n, nematic phase; s_{Ad}, interdigitated smectic A phase; i, isotropic liquid. [b] Data taken from the first (for **AnCN**) or second (for **PAnCN**) heating scan. [c] Data taken from the first cooling scan.

butyne)s was insensitive to the type of catalysts [cis content (%): $MoCl_5$, 77; WCl_6, 76],[29] and Akagi et al. reported that $MoCl_5$−Ph_4Sn gave trans-rich polyacetylenes.[6] The stereostructure of the poly(cyanoalkynes), however, changes with the length of the methylene spacers: **PA2CN** is cis-rich whereas **PA8CN** is trans-rich.

The solubility of WCl_6 in toluene is poor. However, when the metal halide was admixed with the ether solvents, macroscopically homogeneous black-blue solutions formed. The ether solvents thus may have formed some sort of complexes with the W catalysts; in other words, the solvents may be actually serving as cocatalysts in the cyanoalkyne polymerizations. The molecular interaction between THF and the catalysts is so strong that it initiated the THF polymerization. Because tungsten "likes" oxygen,[47] the interaction between WCl_6 and dioxane may generate metal−oxo complexes,[48] which may be the actual active species that initiated the cyanoalkyne polymerizations.[24] Although the THF polymerization was regarded as a complication because of the trouble in separating the large amount of the solvent polymer, an intriguing possibility is that segmented amphiphilic poly(acetylene-*co*-THF)s might be synthesized using the W catalysts under optimized reaction conditions, which is currently pursued in our laboratories. The copolymerization, if it does occur, would also shed light on the mechanisms of the acetylene polymerizations.

We have further found that the tungsten−dioxane catalysts can also initiate polymerizations of the acetylene monomers with hydroxy (−OH) and carboxy (CO_2H) functionalities.[49] In other words, we have developed a general polymerization system for synthesizing polyacetylenes containing different functional groups using the readily available WCl_6-based catalysts. Our work thus widens the scope of the applicability of the simple metal−halide catalysts and opens a new avenue for the development of functional polyacetylenes.

The mesogen-containing poly(cyanoalkynes) show interesting mesomorphic properties, which can be summarized as follows: (i) The rigid backbone perturbs the ordering of the mesogenic pendants. The **PBnCN** with a highly rigid poly(phenylacetylene) backbone is nonmesomorphic, whereas the **PAnCN** with a less stiff poly(1-alkyne) main chain is liquid crystalline. This finding is of fundamental importance, which may help guide the molecular design of mesomorphic conjugated polymers. (ii) The long flexible methylene spacer favors better ordering of the mesogenic units. The **PA2CN** with a shorter spacer exhibits a monotropic nematic mesophase, whereas the **PA8CN** with a longer spacer displays an enantiotropic interdigitated smectic A mesophase over a wide temperature range (>100 °C). (iii) Although **PAnCN**s are side-chain liquid crystalline polymers, **PA8CN** displays the banded structures. The in-domain banded structures form during the transit of the bâtonnets to the focal-conic fan textures without the help of any external forces, and the large-scale banded morphology is induced by mechanical shearing. Thus the rigidity of the polyacetylene backbones is a double-edged sword. It distorts the packing arrangements of the mesogenic pendants when the flexible spacers are too short. On the other hand, it induces novel molecular alignments such as the banded structures when the spacer is long enough. This provides attractive opportunities for polymer scientists and materials engineers to exercise the molecular engineering endeavor to design the "right" molecular structures to maximize the positive effects of the rigid polymer backbones. Such research efforts may eventually lead to the development of a new class of advanced materials: side-chain liquid crystalline polymers with *rigid* backbones.

The formation of the in-domain banded structures may stem from the stereochemical effect. Noting that **PA8CN** consists of cis and trans stereoisomers, the stereosegments or -blocks with different conformations may add to the interdigitated layers in different orientations. This would result in the formation of the microdomains with different refractive indexes, thus generating the banded textures of different color. Compared with flexible polymer backbones, the unique feature of stiff-chain polymers is their alignability by external forces.[50] The band formation after the mechanical shearing may originate from the relaxation of the forcefully extended rigid polyacetylene backbones back to their most probable conformations, in view of the observation that all the bands are perpendicular to the direction of the applied shear force. Although the shear-induced band texture is a ubiquitous morphology seen in main-chain liquid crystalline polymers,[42] the band formation without shearing in the transit to the focal-conic fan texture is an intriguing phenomenon and deserves further investigation. Understanding the phenomenon may widen and deepen our knowledge on how the molecular layers are added to the focal-conic domains[40] and may provide us with a microphotographic "eye" to experimentally "see" the dynamic processes of the growth of the focal-conic fan texture, one of the most frequently observed textures in polymer liquid crystals.

Experimental Section

Materials and Instruments. Dioxane (Aldrich), THF (Lab-Scan), and toluene (BDH) were dried over 4 Å molecular

sieves and distilled from sodium benzophenone ketyl immediately prior to use. Dichoromethane (Lab-Scan) and carbon tetrachloride (Aldrich) were distilled over calcium hydride. 4-Pentynoic, 5-hexynoic, and 10-undecynoic acids were purchased from Farchan Laboratory. 4′-Hydroxy-4-biphenylcarbonitrile, DCC, DMAP, tungsten(VI) chloride, tetraphenyltin, bicyclo[2.2.1]hepta-2,5-diene molybdenum tetracarbonyl [Mo(nbd)$(CO)_4$], mesitylene tungsten tricarbonyl, palladium chloride (all from Aldrich), and molybdenum(V) chloride (Acros and Aldrich) were used as received without further purification.

The infrared spectra were recorded on a Perkin-Elmer 16 PC FT-IR spectrophotometer. The ^{1}H and ^{13}C NMR spectra were measured on a Bruker ARX 300 NMR spectrometer using chloroform-*d* or DMSO-d_8 as solvent. The chemical shifts are reported in ppm on the δ scale, and tetramethylsilane (TMS) or chloroform-*d* was used as internal reference for the NMR analysis. The UV spectra were recorded on a Milton Roy Spectronic 3000 Array spectrophotometer, and the mass spectra were measured on a Finnigan TSQ 7000 triple quadrupole mass spectrometer operating in an EI mode.

The molecular weights of the polymers were estimated by GPC using a Waters Associates liquid chromatograph equipped with a Waters 510 HPLC pump, a Rheodyne 7725i injector with a stand kit, a set of Styragel columns (HT3, HT4, and HT6; molecular weight range 10^2-10^7), a column temperature controller, a Waters 486 wavelength-tunable UV−vis detector, a Waters 410 differential refractometer (RI detector), and a system DMM/scanner with 8 channel scanner option. All the polymer solutions were prepared in THF (ca. 2 mg/mL) and filtered through 0.45-μm PTFE syringe-type filters before being injected into the GPC system. THF was used as the eluent at a flow rate of 1.0 mL/min. The column temperature was maintained at 40 °C, and the working wavelength of the UV detector was set at 254 nm. A set of 12 monodisperse polystyrene standards (Waters; molecular weight range 982−1 945 300) were used for calibration purposes.

Under a nitrogen atmosphere, the TGA analysis was performed on a Perkin-Elmer TGA 7 at a heating rate of 20 °C/min, and the DSC thermograms were recorded on a Setaram DSC 92 at a heating or cooling rate of 10 °C/min. An Olympus BX 60 POM equipped with a Linkam TMS 92 hot stage was used in cross-polarized mode for the visual observation of the thermal behavior of the monomers and polymers.

The wide-angle X-ray diffraction patterns were recorded on a Philips PW1830 powder diffractometer with a graphite monochromator using 1.5406 Å Cu Kα wavelength at room temperature (scan rate: 0.01°/s; scan range: 2-30°). The polymer samples for the X-ray diffraction experiments were prepared by freezing the molecular arrangements in the liquid crystalline states by liquid nitrogen. A typical experimental procedure for the sample preparation is given below: A powdery sample of **PA8CN** sandwiched between a single-crystal silicon wafer and an IR-grade sodium chloride pellet was heated on the hot stage to its isotropic state (225 °C), at which the heating was continued for 5 min. After cooling at a rate of 10 °C/min to its liquid crystalline state (165 °C) and annealing there for 5 min, the wafer was quickly thrown into a liquid nitrogen Dewar flask. The wafer was taken out from the flask, naturally warmed to room temperature, and rinsed with deionized water to remove the sodium chloride cover. The polymer film thus obtained on the silicon wafer was dried in a vacuum oven, which was then used for the X-ray diffraction measurement.

Monomers Synthesis. AnCNs were prepared via the esterification of the *n*-alkynoic acids with 4′-hydroxy-4-biphenylcarbonitrile by three different synthetic routes (cf. Scheme 1). A typical experimental procedure for preparing **A2CN** via the DCC/DMAP route is given below: 4′-Hydroxy-4-biphenylcarbonitrile (1.95 g, 10 mmol), 4-pentynoic acid (1.10 g, 11 mmol), and DMAP (60 mg, 0.45 mmol) were dissolved in 250 mL of dry dichloromethane in a 500-mL two-necked flask under nitrogen. The solution was cooled to 0−5 °C with an ice−water bath, to which 2.27 g of DCC (11 mmol) in 50 mL of dichloromethane was added with stirring via a dropping funnel with a pressure-equalization arm. The reaction mixture was stirred overnight. After filtering out the crystalline urea byproduct, the solution was concentrated by a rotary evaporator. The product was purified by column chromatography using chloroform as the eluent followed by the recrystallization from ethanol. The cyanoalkyne monomers with other lengths of the methylene spacers, i.e., **A3CN** and **A8CN**, were prepared under similar reaction conditions.

Characterization Data. A2CN: white crystal; yield 76%; ^{1}H NMR (300 MHz, $CDCl_3$) δ (ppm) 7.67−7.50 (m, 6H, Ar), 7.17−7.14 (m, 2H, Ar), 2.80 (t, 2H, CH_2CO_2), 2.58 (dt, 2H, $CH_2C{\equiv}C$), 1.99 (t, 1H, C≡CH); ^{13}C NMR (75 MHz, $CDCl_3$), δ (ppm) 170.8 (CO_2), 151.7, 145.4, 137.7, 133.3, 129.0, 128.4, 122.9 (aromatic carbons), 119.5 (C≡N), 111.8 (Ar), 82.6 (*C*≡CH), 70.2 (C≡*C*H), 34.2 (*C*H_2CO_2), 15.1 (*C*H_2C≡C); IR (KBr) ν (cm^{-1}) 3244 (s, ≡C−HH), 2231 (s, C≡C and C≡N), 1746 (s, C═O), 1305 (m, ≡C−H), 710 (m, ≡C−H); MS (EI): *m*/*e* 275.1 (M^+, calcd 275.1), 195.1 {[M − (HC≡C(CH_2)$_2$C═O)]$^+$, calcd 195.1}.

A3CN: white crystal; yield 73%; ^{1}H NMR (300 MHz, $CDCl_3$) δ (ppm) 7.74−7.58 (m, 6H, Ar), 7.23−7.20 (m, 2H, Ar), 2.78 (t, 2H, CH_2CO_2), 2.38 (dt, 2H, $CH_2C{\equiv}C$), 2.00 (m, 3H, CH_2 and C≡CH); ^{13}C NMR (75 MHz, $CDCl_3$) δ (ppm) 171.5 (CO_2), 151.1, 144.7, 136.9, 132.6, 128.3, 127.7, 122.3 (aromatic carbons), 118.8 (C≡N), 83.0 (*C*≡CH), 69.5 (C≡*C*H), 32.9 (*C*H_2CO_2), 23.4 (CH_2), 17.8 (*C*H_2C≡C); IR (KBr) ν (cm^{-1}) 3262 (s, ≡C−H), 2226.0 (s, C≡C and C≡N), 1754 (s, C═O), 1344 (m, ≡C−H), 686 (m, ≡C−H); MS (EI): *m*/*e* 289.1 (M^+, calcd 289.1), 195.0 {[M − (HC≡C(CH_2)$_3$C═O)]$^+$, calcd 195.1}, 94.9 {[M − (O-biph-CN)]$^+$, calcd 95.0}.

A8CN: white crystal; yield 81%; ^{1}H NMR (300 MHz, $CDCl_3$) δ (ppm) 7.74−7.57 (m, 6H, Ar), 7.21−7.18 (m, 2H, Ar), 2.59 (t, 2H, CH_2CO_2), 2.19 (dt, 2H, $CH_2C{\equiv}C$), 1.94 (t, 1H, C≡CH), 1.77 (quintet, 2H, CH_2), 1.54 (quintet, 2H, C*H*$_2$CH$_2$C≡C), 1.46−1.24 [m, 8H, $(CH_2)_4$]; ^{13}C NMR (75 MHz, $CDCl_3$) δ (ppm) 172.8 (CO_2), 151.9, 145.5, 137.4, 133.3, 129.0, 128.3, 123.0 (aromatic carbons), 119.5 (C≡N), 85.3 (*C*≡CH), 68.8 (C≡*C*H), 35.04 (*C*H_2-CO_2), 29.8, 29.7, 29.6, 29.3, 29.1 [$(CH_2)_5$ carbons], 25.5 (C*H*$_2$-CH_2CO_2), 19.0 (*C*H_2C≡C); IR (KBr) ν (cm^{-1}) 3062 (s, ≡C−H), 2226.0 (s, C≡C and C≡N), 1754 (s, C═O), 1322 (m, ≡C−H), 680 (m, ≡C−H); MS (EI): *m*/*e* 359.2 (M^+, calcd 359.2), 195.0 {[M − (HC≡C(CH_2)$_8$C═O)]$^+$, calcd 195.1}, 165.5 {[M − (O-biph-CN)]$^+$, calcd 165.1}.

Polymerization. All the polymerization reactions and manipulations were carried out under a nitrogen atmosphere using either an inert-atmosphere glovebox (Vacuum Atmospheres) or Schlenk techniques in a vacuum line systems, except for the purification of the polymers, which was done in an open atmosphere. A typical experimental procedure for polymerizing **A8CN** is given below: Into a baked 20-mL Schlenk tube with a three-way stopcock on the sidearm was added 287.4 mg of **A8CN**. The tube was evacuated under vacuum and then flushed with dry nitrogen three times through the sidearm. Dioxane (2 mL) was injected into the tube through a septum to dissolve the monomer. The catalyst solution was prepared in another tube by dissolving 7.9 mg of WCl_6 and 8.6 mg of Ph_4Sn in 2 mL of dioxane, which was aged for 10 min at room temperature. The monomer solution was then transferred to the catalyst solution using a hypodermic syringe. The polymerization mixture was stirred under nitrogen at room temperature for 24 h. The mixture was then diluted with 5 mL of dioxane and added dropwise to 200 mL of methanol through a cotton filter with stirring. The precipitate was allowed to stay overnight, which was then filtered off by a Pyrex Gooch crucible, washed with methanol, and dried in a vacuum oven at 40 °C to a constant weight. Yield: 22.0%, yellow powdery solid. M_w: 36 100, M_w/M_n: 2.2 (GPC, polystyrene calibration). ^{1}H NMR (300 MHz, $CDCl_3$), δ (ppm) 7.71−6.95 (Ar−H and trans HC═C), 5.85 (cis HC═C), 2.51 (CH_2CO_2), 2.18 ($CH_2C{=}C$), 1.71 (C*H*$_2$CH$_2$CO$_2$), 1.34 [$(CH_2)_5$]. ^{13}C NMR (75 MHz, $CDCl_3$), δ (ppm) 171.9 (C═O), 151.1, 132.6, 128.2, 127.5, 122.2, 118.7 (C≡N), 111.2, 34.3, 29.3, 24.9. IR (KBr), ν (cm^{-1}): 2228 (C≡N), 1756 (C═O). UV (THF, 2.64 × 10^{-5} mol/L), λ_{max}: 273.2 nm (ϵ_{max}: 2.54 × 10^4 mol^{-1} L cm^{-1}).

Acknowledgment. This project was in part supported by the Hong Kong RGC Earmarked Grants awarded to B.Z.T. (HKUST597/95P and HKUST6149/97P). This project also benefited from the support of the Hong Kong Industry Department, the Nanostructure Materials and Technology Joint Laboratory of HKUST-CAS (Chinese Academy of Sciences), the Advanced Materials Research Institute of HKUST, and the Technology Resource International Corp., Alpharetta, GA.

References and Notes

(1) (a) Petty, M. C.; Bryce, M. R.; Bloor, D. *An Introduction to Molecular Electronics*; Edward Arnold: London, 1995. (b) *Liquid-Crystalline Polymers*; Weiss, R. A., Ober, C. K., Eds.; American Chemical Society: Washington, DC, 1990. (c) Collings, P. J. *Liquid Crystals: Nature's Delicate Phase of Matter*; Princeton University Press: Princeton, NJ, 1990. (d) *Liquid Crystalline Polymer Systems: Technological Advances*; Isayev, A. I., Kyu, T., Cheng, S. Z. D., Eds.; American Chemical Society: Washinton, DC, 1996. (e) *Optical Effects in Liquid Crystals*; Janossy, I., Ed.; Kluwer: Dordrecht, 1991. (f) *Conjugated Polymeric Materials: Opportunities in Electronics, Optoelectronics and Molecular Electronics*; Bredas, J. L., Chance, R. R., Eds.; Kluwer: Boston, 1990. (g) *Polymeric Liquid Crystals*; Blumstein, A., Ed.; Plenum: New York, 1985. (h) Chien, J. C. W. *Polyacetylene*; Academic Press: New York, 1984.

(2) (a) Sutherland, R. L. *Handbook of Nonlinear Optics*; Marcel Dekker: New York, 1996. (b) *Organic, Metallo-Organic, and Polymeric Materials for Nonlinear Optical Applications*; Marder, S. R., Perry, J. W., Eds.; SPIE: Washington, DC, 1994. (c) *Nonlinear Optical Properties of Advanced Materials*; Etemad, S., Ed.; SPIE: Washington, DC, 1993. (d) *Conjugated Polymers: the Novel Science and Technology of Highly Conducting and Nonlinear Optically Active Materials*; Bredas, J. L., Silbey, R., Eds.; Kluwer: Dordrecht, The Netherlands, 1991. (e) Prasad, P. N.; Williams, D. J. *Introduction to Nonlinear Optical Effects in Molecules and Polymers*; Wiley: New York, 1990.

(3) (a) Tang, B. Z.; Peng, H.; Leung, S. M.; Yu, N.-T.; Hiraoka, H.; Fok, M. W. In *Materials for Optical Limiting II*; Hood, P., Pachter, R., Lewis, K., Perry, J. W., Hagan, D., Sutherland, R., Eds.; Materials Research Society: Pittsburgh, PA, 1997; p 69. (b) Tang, B. Z.; Peng, H.; Leung, S. M.; Au, C. F.; Poon, W. H.; Chen, H.; Wu, X.; Fok, M. W.; Yu, N.-T.; Hiraoka, H.; Song, C.; Fu, J.; Ge, W.; Wong, G.; Monde, T.; Nemoto, F.; Su, K. C. *Macromolecules* **1998**, *31*, 103. (c) Tang, B. Z.; Leung, S. M.; Peng, H.; Yu, N.-T.; Su, K. C. *Macromolecules* **1997**, *30*, 2848. (d) Tang, B. Z.; Yu, N.-T.; Ge, W.; Wu, X. U.S. Patent Appl. No. 08/563,577, 1995. (e) Kojima, Y.; Matsuoka, T.; Sato, N.; Takahashi, H. *Macromolecules* **1995**, *28*, 2893. (f) *Materials for Optical Limiting*; Crane, R., Ed.; Materials Research Society: Pittsburgh, PA, 1995. (g) *Nonlinear Optical Materials for Switching and Limiting*; Soileau, M. J., Ed.; SPIE: Washington, DC, 1994. (h) Tutt, L. W.; Boggess, T. F. *Prog. Quantum Electron.* **1993**, *17*, 299.

(4) (a) Ginsburg, E. J.; Gorman, C. B.; Grubbs, R. H. In *Modern Acetylene Chemistry*; Stang, P. J., Diederich, F., Eds.; VCH: New York, 1995; Chapter 10. (b) Shirakawa, H.; Masuda, T.; Takeda, K. In *The Chemistry of Triple-Bonded Functional Groups, Supplement C2*; Patai, S., Ed.; Wiley: New York, 1994; Chapter 17. (c) Schrock, R. R. *Acc. Chem. Res.* **1990**, *23*, 158. (d) Masuda, T.; Higashimura, T. *Adv. Polym. Sci.* **1987**, *81*, 121. (e) Gibson, H. W.; Pochan, J. M. In *Encyclopedia of Polymer Science and Engineering*; Kvoschwitz. J. I., Ed.; Wiley: New York, 1985; p 44.

(5) (a) Lee, H. J.; Shim, S. C. *J. Polym. Sci., Part A: Polym. Chem.* **1994**, *32*, 2437. (b) Yang, M.; Zheng, M.; Furlani, A.; Russo, M. V. *J. Polym. Sci., Part A: Polym. Chem.* **1994**, *32*, 2709. (c) Gai, Y.-S. *Chem. Commun.* **1994**, 327. (d) Rossitto, F. C.; Lahti, P. M. *Macromolecules* **1993**, *26*, 6308. (e) Lee, H.; Shim, S. C. *Chem. Commun.* **1993**, 1421. (f) Nishide, H.; Yoshioka, N.; Inagaki, K.; Kaku, T.; Tsuchida, E. *Macromolecules* **1992**, *25*, 569. (g) Gal. Y.-S.; Jung, B.; Lee, W.-C.; Choi, S.-K. *J. Polym. Sci., Part A: Polym. Chem.* **1992**, *30*, 2657. (h) Masuda, T.; Kawai, M.; Higashimura, T. *Polymer* **1982**, *23*, 744. (i) Katz, T. J.; Lee, S. J. *J. Am. Chem. Soc.* **1980**, *102*, 422. (j) Kiyashkina, Zh. S.; Pomogailo, A. D.; Kuzayev, A. I.; Lagodzinskaya, G. V.; Dyachkovskii, F. S. *J. Polym. Sci., Polym. Symp.* **1980**, *68*, 13.

(6) (a) Akagi, K.; Shirakawa, H. *Macromol. Symp.* **1996**, *104*, 137. (b) Oh, S.−Y.; Akagi, K.; Shirakawa, H. *Macromolecules* **1993**, *26*, 6203.

(7) (a) Ho, T. H.; Katz, T. J. *J. Mol. Catal.* **1985**, *28*, 359. (b) Carlini, C.; Chien, J. C. W. *J. Polym. Sci., Polym. Chem. Ed.* **1984**, *22*, 2749. (c) Deits, W.; Cukor, P.; Rubner, M.; Jopson, H. *Ind. Eng. Chem. Prod. Res. Dev.* **1981**, *20*, 696. (d) Hankin, A. G.; North, A. M. *Trans. Faraday Soc.* **1967**, *63*, 1525. (e) MacNulty, B. J. *Polymer* **1967**, *63*, 1525. (f) Mison, A.; Noughchi, H.; Noda, S. *J. Polym. Sci., Polym. Lett. Ed.* **1966**, *4*, 985.

(8) Tang, B. Z.; Kong, X.; Wan, X.; Feng, X.-D. *Macromolecules* **1997**, *30*, 5620.

(9) (a) Carbrea, I.; Krongauz, V. *Nature* **1987**, *326*, 582. (b) Carbrea, I.; Krongauz, V.; Rinsdorf, H. *Angew. Chem., Int. Ed. Engl.* **1987**, *26*, 1178. (c) Goldburt, E.; Schbvartsman, F.; Krongauz, V. *Macromolecules* **1984**, *17*, 1876 and 1225. (d) Krongauz, V. A.; Goldburt, E. S. *Macromolecules* **1981**, *14*, 1382. (e) Interestingly, we also observed swelling-induced optical anisotropy in our **PBnCN** systems, details of which will be published by X. Kong and B. Z. Tang in due course.

(10) Maughon, B. R.; Weck, M.; Mohr, B.; Grubbs, R. H. *Macromolecules* **1997**, *30*, 257.

(11) Masuda, T.; Tang, B. Z.; Tanaka, A.; Higashimura, T. *Macromolecules* **1986**, *19*, 1459 and references therein.

(12) (a) Yashima, E.; Matsushima, T.; Okamoto, Y. *J. Am. Chem. Soc.* **1997**, *119*, 6345. (b) Tabata, M.; Tanaka, Y.; Sadahiro, Y.; Sone, T.; Yokota, K.; Miura, I. *Macromolecules* **1997**, *30*, 5200. (c) Aoki, T.; Shinohara, K.; Kaneko, T.; Oikawa, E. *Macromolecules* **1996**, *29*, 4192. (d) Kishmoto, Y.; Miyatake, T.; Ikariya, T.; Noyori, R. *Macromolecules* **1996**, *29*, 5054. (e) Yashima, E.; Huang, S.; Okamoto, Y. *J. Chem. Soc., Chem. Commun.* **1994**, 1811.

(13) (a) Zhang, X.; Ozcayir, Y.; Feng, C.; Blumstein, A. *Polym. Prepr.* **1990**, *31* (1), 597. (b) Furniss, B. S.; Hannaford, A. J.; Smith, P. G.; Tatchell, A. R. *Vogel's Textbook of Practical Organic Chemistry*, 5th ed.; Longman: Essex, 1989.

(14) Larock, R. C. *Comprohensive Organic Transformations: A Guide to Functional Group Preparations*; VCH: New York, 1989.

(15) The detailed crystal structure data will be published by X. Kong, I. D. Williams, and B. Z. Tang in a separate paper.

(16) Cf. group dipole moment: CH_3O 1.3, CO_2H 1.7, CN 4.0. Molecule dipole moment: $C_6H_5OCH_2CH_3$ 1.45, $C_6H_5CO_2CH_2$-CH_3 2.00, C_6H_5CN 4.18. Data taken from ref 17.

(17) (a) Carey, F. A.; Sundberg, R. J. *Advanced Organic Chemistry*, 3rd ed.; Plenum: New York, 1990. (b) *CRC Handbook of Chemistry and Physics*, 75th ed.; Lide, D. R., Ed.; CRC Press: Boca Raton, FL, 1994.

(18) Masuda, T.; Kawai, M.; Higashimura, T. *Polymer* **1982**, *23*, 744.

(19) (a) Iwamura, H.; McKelvey, R. D. *Macromolecules* **1988**, *21*, 3386. (b) Le Moigne, J.; Hilberer, A.; Strazielle, C. *Macromolecules* **1992**, *25*, 6705.

(20) Dreyfuss, P.; Dreyfuss, M. P.; Pruckmayr, G. In *Concise Encyclopedia of Polymer Science and Engineering*; Kroschwitz, J. I., Ed.; Wiley: New York, 1990; p 1175.

(21) Okamura, S.; Nakajima, A.: Onogi, S.; Kawai, H.; Nishijima, Y.; Higashimura, T.; Ise, N. *Kobunshi Kagaku Joron (Introduction to Polymer Chemistry)*, 2nd ed.; Kagaku Dojin: Kyoto, 1994.

(22) Tang B. Z.; Kotera, N. *Macromolecules* **1989**, *22*, 4388.

(23) (a) Calderazzo, F.; Ercoli, R.: Natta, G. In *Organic Syntheses via Metal Carbonyls*; Wender, I., Piero, P., Eds.; Willey: New York, 1968; Vol. 1. (b) Kreiter, C. G. *Adv. Organomet. Chem.* **1986**, *26*, 297.

(24) (a) Masuda, T.; Izumikawa, H.; Sumi, Y.; Higashimura, T. *Macromolecules* **1996**, *29*, 1167. (b) Nakano, M.; Masuda, T.; Higashimura, T. *Macromolecules* **1994**, *27*, 1344. (c) Masuda, T.; Mishima, K.; Fujimori, J.-I.; Nishida, M.; Muramatsu, H.; Higashimura, T. *Macromolecules* **1992**, *25*, 1401.

(25) (a) Roeges, N. P. G. *A Gguide to the Complete Interpretation of Infrared Spectra of Organic Structures*; Wiley: New York, 1994; p 104. (b) Lin-Vien, D.; Colthup, N. B.; Fateley, W. G.; Grasselli, J. G. *The Handbook of Infrared and Raman Characteristic Frequencies of Organic Molecules*; Academic Press: Boston, 1991.

(26) Okano, Y.; Masuda, T. Higashimura, T. *J. Polym. Sci., Polym. Chem. Ed.* **1985**, *23*, 2537.

(27) (a) Simionescu, C. I.; Percec, V.; Dumitrescu, S. *J. Polym. Sci., Polym. Chem. Ed.* **1977**, *15*, 2497. (b) Simionescu, C. I.; Percec, V. *J. Polym. Sci., Polym. Symp.* **1980**, *67*, 43. (c) Cianciusi, A. M.; Furlani, A.; Ginestra, A. L.; Russo, M. V.; Palyi, G.; Vizi-Orosz, A. *Polymer* **1990**, *31*, 1568.
(28) (a) Tang, B. Z.; Poon, W. H.; Leung, S. M.; Leung, W. H.; Peng, H. *Macromolecules* **1997**, *30*, 2209. (b) Tang, B. Z.; Poon, W. H. U.S. Patent Appl. No. 08/821,433, 1997.
(29) Masuda, T.; Okano, Y.; Tamura, K.; Higashimura, T. *Polymer* **1985**, *26*, 793.
(30) Masuda, T.; Higashimura, T. *Acc. Chem. Res.* **1984**, *17*, 51.
(31) (a) Tonelli, A. E. *NMR Spectroscopy and Polymer Microstructure*; VCH: New York, 1989. (b) *High-Resolution NMR Spectroscopy of Synthetic Polymers in Bulk*; Komoroski, R. A., Ed.; VCH: Deerfield Beach, FL, 1986.
(32) (a) Masuda, T.; Izumikawa, H.; Misumi, Y.; Higashimura, T. *Macromolecules* **1996**, *29*, 1167. (b) Masuda, T.; Okano, Y.; Kuwane, Y.; Higashimura, T. *Polym. J.* **1980**, *12*, 907. (c) Okano, Y.; Masuda, T.; Higashimura, T. *Polym. J.* **1982**, *14*, 477.
(33) (a) *Handbook of Spectroscopy*; Robinson, J. W., Ed.; CRC Press: Boca Raton, FL, 1981. (b) Silverstein, R. M.; Bassler, G. C.; Morrill, T. C. *Spectrometric Identification of Organic Compounds*, 5th ed.; Wiley: New York, 1991.
(34) Masuda, T.; Tang, B. Z.; Higashimura, T.; Yamaoka, H. *Macromolecules* **1985**, *18*, 2369.
(35) Tang, B. Z.; Wan, X.; Kwok, H, S. *Eur. Polym. J.*, in press.
(36) Tang, B. Z.; Peng, H.; Leung, S. M. In *Recent Advances in the Chemistry and Physics of Fullerenes and Related Materials*; Kadish, K. M., Ruoff, R. S., Eds.; The Electrochemical Society: Pennington, NJ, 1997; Vol. 4, p 655.
(37) (a) *Handbook of Polymer Degradation*; Hamid, S. H., Amin, M. B., Maadhah, A. G., Eds.; Marcel Dekker: New York, 1992. (b) Allen, N. S.; Edge, M. *Fundamentals of Polymer Degradation and Stabilisation*; Elsevier: London, 1992. (c) *Mechanisms of Polymer Degradation and Stabilisation*; Scott, G., Ed.; Elsevier: London, 1990.
(38) (a) Percec, V.; Pugh, C. In *Side Chain Liquid Crystal Polymers*; McArdle, C. B., Ed.; Chapman & Hall: New York, 1989; Chapter 3. (b) Frosini, A.; Levita, G.; Lupinacci, D.; Magagnini, P. L. *Mol. Cryst. Liq. Cryst.* **1981**, *66*, 21. (c) Magagnini, P. L. *Makromol. Chem., Suppl.* **1981**, *4*, 223. (d) Hahn, B.; Wendrof, J. H.; Portugall, M.; Ringsdorf, H. *Colloid Polym. Sci.* **1981**, *259*, 875.
(39) (a) Nehring, J.; Saupe, A. *J. Chem. Soc., Faraday Trans. 2* **1972**, *68*, 1. (b) Saupe, A. *Mol. Cryst. Liq. Cryst.* **1973**, *21*, 211.
(40) (a) Demus, D.; Richter, L. *Textures of Liquid Crystals*; Verlag Chemie: Weinheim, 1978. (b) Gray, G. W.; Goodby, J. W. G. *Smectic Liquid Crystals: Textures and Structures*; Leonard Hill: London, 1984. (c) Zhou, Q. F.; Wang X. J. *Liquid Crystalline Polymers*; Science Press: Beijing, 1994.
(41) Dobb, M. G.; Johnson, D. J.; Saville, B. P. *J. Polym. Sci., Polym. Phys. Ed.* **1977**, *15*, 2201.
(42) (a) *Handbook of Liquid Crystal Research*; Collings, P. J., Patel, J. S., Eds.; Oxford University Press: New York, 1997. (b) Donald, A. M.; Windle, A. H. *Liquid Crystalline Polymers*; Cambridge University Press: Cambridge, 1992. (c) Qian, R.; Chen, S. *Makromol. Chem., Makromol. Symp.* **1992**, *53*, 345.
(43) Ge, J. J.; Zhang, A.; McCreight, K. W.; Ho, R.-M.; Wang, S.-Y.; Jin, X.; Harris, F. W.; Cheng, S. Z. D. *Macromolecules* **1997**, *30*, 6498.
(44) (a) Mariani, P.; Rustichelli, F.; Torquati, G. In *Physics of Liquid Crystalline Materials*; Khoo, I.-C., Simoni, F., Eds.; Gordon & Breach Science: New York, 1991; Chapter 1. (b) *Liquid Crystalline Order in Polymers*; Blumstein, A., Hsu, E. C., Eds.; Academic Press: New York, 1978. (c) *Liquid Crystalline and Mesomorphic Polymers*; Shibaev, V., Lam, L., Eds.; Springer-Verlag: New York, 1994.
(45) Kato, T.; Kubota, Y.; Uryu, T.; Ujiie, S. *Angew. Chem., Int. Ed. Engl.* **1997**, *36*, 1617.
(46) (a) Le Barny, P.; Dubois, J.-C.; Friedrich, C.; Noel, C. *Polym. Bull.* **1986**, *15*, 341. (b) Noel, C.; Navard, P. *Prog. Polym. Sci.* **1991**, *16*, 55. (c) Deschenaux, R.; Turpin, F.; Guillon, D. *Macromolecules* **1997**, *30*, 3759. (d) Jojansson, G.; Percec, V.; Ungar, G.; Smith, K. *Chem. Mater.* **1997**, *9*, 164 and references therein.
(47) Cotton, F. A.; Wilkinson, G. *Advanced Ingorganic Chemistry*, 5th ed.; Wiley: New York, 1988.
(48) (a) Persson, C.; Anderson, C. *Polyhedron* **1992**, *11*, 847. (b) Dreisch, K.; Andersson, C.; Stalhandske, C. *Polyhedron* **1991**, *10*, 2417. (c) Gibson, V. C.; Kee, T. P.; Shaw, A. *Polyhedron* **1988**, *7*, 579.
(49) Wan, X.; Kong, X.; Tang, B. Z. Manuscript in preparation.
(50) (a) Ballauff, M. *Angew. Chem., Int. Ed. Engl.* **1989**, *28*, 253. (b) Tsvetkov, V. N. *Rigid-Chain Polymers*; Consultants Bureau: New York, 1989. (c) *The Materials Science and Engineering of Rigid-Rod Polymers*; Adams, W. W., Eby, R. K., McLemore, D. E., Eds.; Materials Research Society: Pittsburgh, PA, 1989. (d) *Toughened Plastics I: Science and Engineering*; Riew, C. K., Kinloch, A. J., Eds.; American Chemical Society: Washington, DC, 1993.

MA971672L